Heat transfer enhancement with a piezoelectric fan

X.L. Zhong[a], K.C. Chan[a,] *, S.C. Fu[b], L.Q. Wang [a], Christopher Y.H. Chao[c]

[a]Department of Mechanical Engineering, The University of Hong Kong, Hong Kong, China

[b]Department of Building Environment and Energy Engineering, The Hong Kong Polytechnic University, Hong Kong, China

[c]Department of Building Environment and Energy Engineering and Department of Mechanical Engineering, The Hong Kong Polytechnic University, Hong Kong, China

* Corresponding Author Tel.: +(852) 39102155

E-mail address: mekcchan@hku.hk

Address: Department of Mechanical Engineering, The University of Hong Kong, Hong Kong, China

Highlights

- Geometrical optimization enhances the piezoelectric fan cooling effect by 70%.
- Fan location and channel configuration are important for heat transfer enhancement.
- By balancing the streamwise velocity and spanwise mixing, the performance of piezoelectric fan cooling can be maximized.

Abstract

Speedy technology development requires more advanced cooling devices than before. Piezoelectric fan cooling has the great potential to contribute to future electronic cooling for its compact size and high energy efficiency. However, the cooling capacity of piezoelectric fan cooling has not yet been fully unfolded; it is in urgent need to maximize its cooling performance to catch up with the industry demand. In this work, we aim to increase the heat transfer performance by varying the piezoelectric fan location and channel configuration. The effect of fan location is firstly studied. By tuning the fan position, a higher streamwise velocity is achieved, thus increasing the heat transfer. A fan inserted into the channel achieves a 55% enhancement on the Nusselt number, higher than the case of an outside-channel fan, which is the commonly adopted configuration. On top of this, the effect of the channel configuration is explored. Both expansion and contraction configurations benefit the heat transfer, and an optimized one increases the cooling effect by 70%. The fan motion is captured by a high-speed camera. Flow visualization is used to investigate the flow pattern. The channel streamwise fluid velocity is examined. It is found that the contraction configuration boosts the streamwise velocity and generates a jet flow pattern at the channel outlet. The expansion configuration significantly alters the flow motion with more vortices in a longer transmission distance, yielding a stronger spanwise mixing. The findings demonstrate that geometrical optimization can substantially enhance the heat transfer performance of the piezoelectric fan, thus paving the way for tackling the urgent cooling requirement.

Keywords

Piezoelectric fan cooling, electronics cooling, heat transfer, flow pattern.

Nomenclature

A	Surface area of the heating plate, m^2
d	The distance between the fan tip and the channel inlet, m
h	Average heat transfer coefficient, W m^{-2} K^{-1}
k	Air thermal conductivity, W m^{-1} K^{-1}
Nu	Nusselt number
Q	Heating power, W

q	Heat flux, W m^{-2}
V	Streamwise velocity, m s^{-1}
w	Channel width, m
δR	Experimental uncertainty
δX_{i}	The uncertainty of one independent variable
ΔT	Temperature difference between the heating plate and environmental air, K
q-q_0	Heat flux enhancement induced by the piezoelectric fan
$\mathrm{Nu}/\mathrm{Nu}_0$	The Nusselt number ratio between piezoelectric fan cooling (fan-on) and natural convection (fan-off)

Greek symbols

θ	Half of the angle of the channel configuration, °
λ	Characteristic length of the channel

Subscripts

0	fan-off condition, or natural-convection condition

1. Introduction

In view of the rapid development of 5G technology, addressing the massive heat generated in limited-size devices has become a growing concern [1,2]. Recalling the history of tackling the heat dissipation problem, using a heat sink is a traditional way to help device cooling [3–5]. However, a heat sink is usually very bulky, and most importantly, its dissipated heat flux is much lower than the generated heat flux in a high-integrated chip. Heatsink modifications, such as changing fin shape and using a material with a higher conductivity, sometimes cannot fulfill the applications that require a high heat dissipation rate, unless the air, the commonly-used heat transfer medium, is altered into liquids [6–9]. The liquid cooling technology was thus developed and significantly increased the surface heat flux [10–14]. However, the introduction of liquids, such as water or oil, poses a great risk of short circuit in case of a liquid leak, which may cause irreversible damages to the electronic system and user. Efforts have been made to look for an alternatively safe and efficient way of high heat flux dissipation. Heat pipe or phase change cooling technology was then invented by adopting an evaporation end near the heat source and placing a condensation end to the surroundings. Both ends were restricted inside a highly conducted copper tube. With the help of the copper tube and phase-change liquid, the heat absorbed is soon transferred and dissipated into the surroundings, leading to a great enhancement in heat transfer compared with the previous single phase cooling technologies [11,15,16]. Another technique is to apply an aeroelastic vortex generator into heat sink channels [17]. Flexible plates are inserted into the channels and interact with the airflow through a flapping motion to generate turbulence. By introducing additional turbulence, it was demonstrated to have as much as 300% enhancement in the heat transfer coefficient [18]. However, since the fluttering motion is driven by the airflow, a fan has to be inserted nearby, which makes the whole setting bulky and a certain amount of power is consumed to overcome the flow pressure loss. The present electronic cooling system urgently demands a more compact, energy-saving system design.

Piezoelectric fan cooling technology simplifies the setting by integrating the fan and aeroelastic plate as a single piezoelectric fan [19,20]. In this technology, the piezoelectric fans are generally placed in front of the inlets of heat sinks or channels. Convective heat transfer occurs on the channel walls as the airflow is introduced into the channel when the fans flutter. The main difference between piezoelectric cooling and aeroelastic vortex generator cooling is that the fluttering motion in the piezoelectric fan cooling is activated

actively by the piezoelectric effect but not passively by the airflow. This provides independent controllability over the fluttering amplitude and frequency, which are no longer controlled limitedly by the airflow velocity. It is reported that the efficiency of piezoelectric fan cooling is about 10 times higher than that of the referenced radial fan [19], showing the promising performance of piezoelectric fan cooling for thermal management. Therefore, with the advantages of piezoelectric fan cooling, including a more compact system, simpler operation and higher efficiency, growing attention is drawn to the development of piezoelectric fan cooling, aiming to further increase its heat transfer performance to meet the current cooling requirement [21–23].

A widely explored factor in previous studies on piezoelectric fan cooling is the fluttering motion of the piezoelectric fan, including the frequency and amplitude. The effects of frequency and amplitude on heat transfer have been examined in [24], and a maximum enhancement of 46% on local heat transfer compared with natural convection is achieved by tuning the fan frequency to the fundamental resonant frequency. Another widely-explored factor is the orientation of the piezoelectric fan [25]. Two conditions are compared, i.e., the fan plane is vertical or parallel to the heat source plane. By changing the orientation, the heat transfer for the system can be improved by 52% [26]. Multi-fan arrays have also been studied [29, 30]. The space, relative orientation and phase variation between the fans have been examined [30, 31]. In-phase fans perform better than counter-phase ones in confined spaces in terms of heat transfer performance [27].

Most of the studies have been focused on the parameters related to the fan or fan arrays, while studies on the effect of the relative geometrical relationship between the fan and the channel are very limited. Geometrical optimization is more efficient and cost-effective than replacing a piezoelectric fan, which is expensive. Therefore, we suggest firstly maximizing the heat transfer performance of a simple combination of a piezoelectric fan and a channel. To our best knowledge, no study has been conducted regarding the comparison of the heat transfer performance between an inside-channel fan and an outside-channel fan. In most application scenarios, the fan is placed outside the channel [28]. It is highly possible that the position of the fan, i.e., placed inside or outside the channel, would significantly affect heat transfer performance. Besides, inspired by the basic knowledge of a jet flow generated by a nozzle [29] and its similar application in the heat sink design [30], it is believed that the channel configuration would have a significant impact on the flow, which would consequently affect the piezoelectric fan cooling. Therefore, optimizing the geometrical arrangement,

including the fan location and the channel configuration, has the potential to boost the heat transfer, which, however, has not yet been studied.

Therefore, the objective of this work is to study how the geometrical arrangement affects the piezoelectric fan cooling, with an expectation of enhancing heat transfer. The effect of fan location on heat transfer is firstly studied. The second step is to study the effect of channel configuration on heat transfer. Two configurations, i.e., contraction and expansion, are considered. The results are fully analyzed from not only the change of the streamwise velocity, but also the flow patterns, as well as the fan motion. Both the results and analysis benefit the development of piezoelectric fan cooling in an electronic system.

2. Experimental method

2.1 Experimental setting, procedures and calculation methods

The experimental setting is shown in Fig. 1(a). A piezoelectric fan was fixed vertically in front of a channel. The piezoelectric fan used in this study was a packaged fan with a pre-attached transformer and signal generator. The blade size was 2 cm × 8 cm. The channel had a default length and height of 15 cm × 8 cm, and its width could be controlled from 1 cm to 2 cm, with an interval of 0.5 cm. The channel had one isothermal-heated sidewall made of a copper plate (5 cm × 15 cm). All experiments were conducted in an air-conditioned environment with the room temperature of 21.5 ± 0.1 °C and humidity of 58%. The surface temperature was set with a difference of 23.5 °C with the indoor temperature by a temperature controller (TC9100, DigiSense, USA). The heating power was monitored by a power meter (RSPM 8213, RS PRO, UK). During the experiment, a parametric study on the channel width (w) and the distance between the fan tip and the channel inlet (d) was firstly performed to obtain the optimal fan location. Then the effect of channel configuration was studied by altering the normal channel configuration to an expansion and contraction one. The channel angle of expansion and contraction configuration was characterized by '2θ' (as shown in Fig. 1(a)), with a negative value in the expansion case and a positive one in the other case.

In each experiment, a background case in which the fan was turned off was firstly conducted, and the heating power Q_0 was recorded. Another experiment was subsequently conducted with the fan-on condition, and the

heating power was recorded as Q. The heat fluxes under the natural convection (fan-off) and fan-on conditions are abstracted as below.

$$q_0 = \frac{Q_0}{A} \tag{1}$$

$$q = \frac{Q}{A} \tag{2}$$

where A is the surface area of the copper plate. Then (q-q_0) is considered as the heat flux enhancement induced by the piezoelectric fan. It is noted that the input power of the piezoelectric fan setting for all cases was measured to be about 2.25 W with a standard deviation of 4.4%. Therefore, all experiments were conducted under the same input power condition.

In order to evaluate the heat transfer enhancement, the Nusselt number, which is a dimensionless number to characterize the convective heat transfer, was used. The Nusselt number is defined as below

$$\mathrm{Nu} = \frac{h\lambda}{k}, \tag{3}$$

$$h = \frac{q}{\Delta T}, \tag{4}$$

where h is the convective heat transfer coefficient, λ and k are the characteristic length and air thermal conductivity, respectively, ΔT is the temperature difference between the heated copper surface and the air. Since both λ and k kept constant between fan-off and fan-on condition, and ΔT was maintained constant at 23.5 °C, the ratio of the Nusselt number at the fan-on condition (Nu) to that at the natural convection (fan-off condition, Nu_0) reduced to:

$$\frac{\mathrm{Nu}}{\mathrm{Nu}_0} = \frac{h}{h_0} = \frac{Q}{Q_0} \tag{5}$$

The measured heat flux under natural convection (fan-off condition) was 415 W/m^2, while the background velocity was essentially 0 m/s.

2.2 Characterization method

The fluttering motion of the piezoelectric fan is captured by a high-speed camera (VEO410, Phantom, Germany). The motion envelope is constructed by superimposing the fan motion within several cycles. The ImageJ software is used to perform the image processing. More details can be referred to our previous work [31].

In this work, we have two ways for velocity measurement. One way is to measure the velocity using an anemometer directly. The velocity at the channel outlet was measured by a one-directional hotwire-based velocimetry (9565-P-NB, TSI, USA) as shown in Fig. 1(b). The probe of the velocimetry was placed at the center of the channel outlet. It is noted that when the fan was turned off, the airflow rate was measured to be 0 m/s, demonstrating that the background airflow was minimal and could be ignored.

The flow pattern in the channel was visualized following the technique described in [32]. In Fig. 1(c), the experimental setup involving the channel and the piezoelectric fan is placed vertically in front of the camera. A flashlight (YN600EX-RT, YONGNUO, CN) is placed on top of the setting, and is connected synchronically with the camera (1000D, Canon, Japan) to generate a sheet light to light up the target plane. To avoid light reflection and have a better contrast, the supporting platform, which is the background for the target plane, is covered by black paper. Smoke wires are placed at the channel inlet and outlet. The smoke wires are made of stainless steel with a diameter of 0.1 mm. Paraffin oil is brushed on the smoke wires and will be evaporated into smoke after turning on the electricity power by a system controller. Subsequently, after triggering the smoke wires, the system controller will send out commands to the camera and flashlight within milliseconds to capture the smoke flow. The captured white smoke flow represents the airflow condition from the position of the smoke wires. By placing the smoke wires at various positions, flow patterns around the piezoelectric fan and inside the channel are captured.

The flow patterns provide us another way for velocity measurement. The smoke traveling distance captured in the images is taken as the propagation distance. The propagation distance is identified easily due to the contrast between the black background and white smoke. The time duration from triggering the smoke to the image capture is recorded, which is 100 ms for open space investigation and 40 ms for channel configuration investigation. With the propagation distance and time, the propagation velocities, including streamwise velocity and spanwise velocity, can be found. Besides, by measuring the size of the smoky area, the propagation area can be obtained.

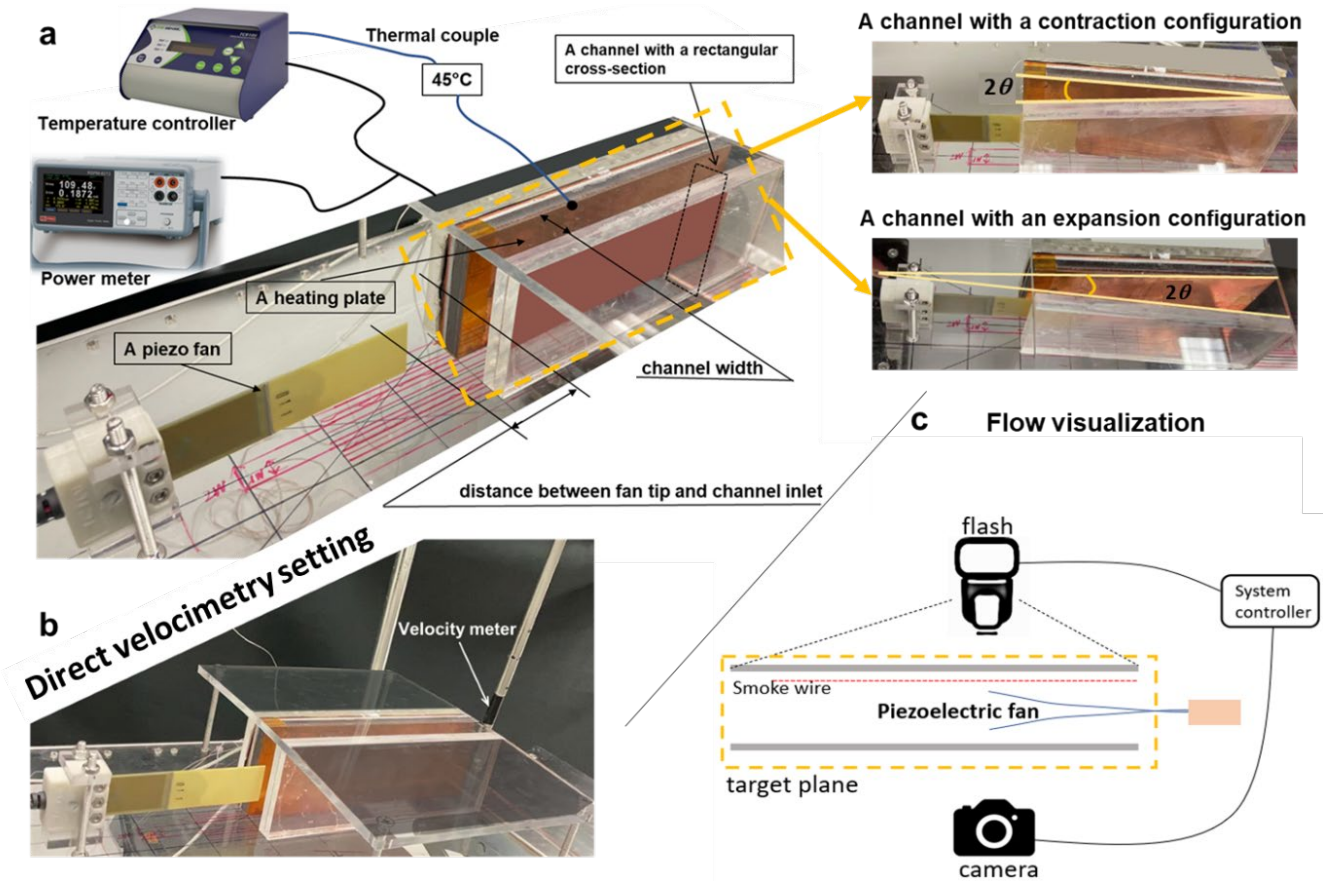

Fig. 1 Experimental setups: (a) Setup for heat transfer experiment; the geometrical restructuring includes different d, different w, and different configuration/angles; (b) Setup for direct velocimetry; (c) Setup for flow visualization, including a camera, flash, the system controller and the setting showing the target plane.

2.3 Uncertainty analysis

The experimental uncertainty is determined [33].

$$\delta R = [\sum_{i}^{N} (\frac{\partial R}{\partial X_i} \delta X_i)^2]^{1/2}$$

where δR is the overall uncertainty and δX_i is the uncertainty induced by a specific variable. The measurement accuracies associated with the experimental components can be referred to our previous work [31]. The measurement of heat flux, q, has a relative uncertainty of 0.2%, while that of Nu is 4%.

3. Results and Discussion

3.1 The motion of the piezoelectric fan and the flow pattern

The frequency of the piezoelectric fan was fixed at 50 Hz, and its tip-to-tip amplitude varied slightly in different cases at around 1.2 cm. Fig. 2(a) shows the projection of the fan motion in multiple cycles.

The flow pattern generated by the piezoelectric fan is also investigated. As shown in Fig. 2(b), the piezoelectric fan is placed on the right-hand side in an open space. There are five smoke wires (three perpendicular and two parallel to the fan) placed around the fan tip, and they will be activated in sequence to show the flow pattern in the specific positions. Fig. 2(c) compares the smoke generated by the three smoke wires perpendicular to the fan showing how the flow patterns vary with different distances from the fan tip. As shown from the smoke wire 1, which is the closest to the fan tip, the fan generates strong and complicated vortices. Moreover, from the smoke wire 2, the vortices weaken as the distance extends and become less complicated with the shrinking vortex size. Besides that, the vortices are clearly driven in the direction that is far away from the fan. In the position where the smoke wire 3 is placed, the vortices disappear and only a slightly forward flow is observed. Therefore, the fan generates a forward flow, and more vortices occur closer to the fan tip. The flow patterns indicated by the two parallel smoke wires with the fan are symmetric, and they represent the flow patterns on two sides of the fan. The spanwise mixing effect is clearly shown, and the effect weakens as the distance from the fan tip increases. The propagation velocities are extracted from the flow pattern and shown in Fig. 2(f-g). Fig. 2(f) shows the streamwise propagation. It is clear that in the open space condition, streamwise propagation induced by the piezoelectric fan is weak and has almost no effect at a distance of 8 cm to the fan tip. The maximum streamwise velocity examined is 0.18 m/s, which occurs 1 cm away from the fan tip. Fig. 2(g) shows the spanwise propagation along the centerline. The centerline is parallel with smoke wires 4 and 5, and starts from the fan head, as indicated in Fig. 2(d). It is clear that the spanwise propagation is symmetric at two sides of the fan. And the strongest propagation is around the fan tip. The maximum spanwise velocity is 0.29 m/s.

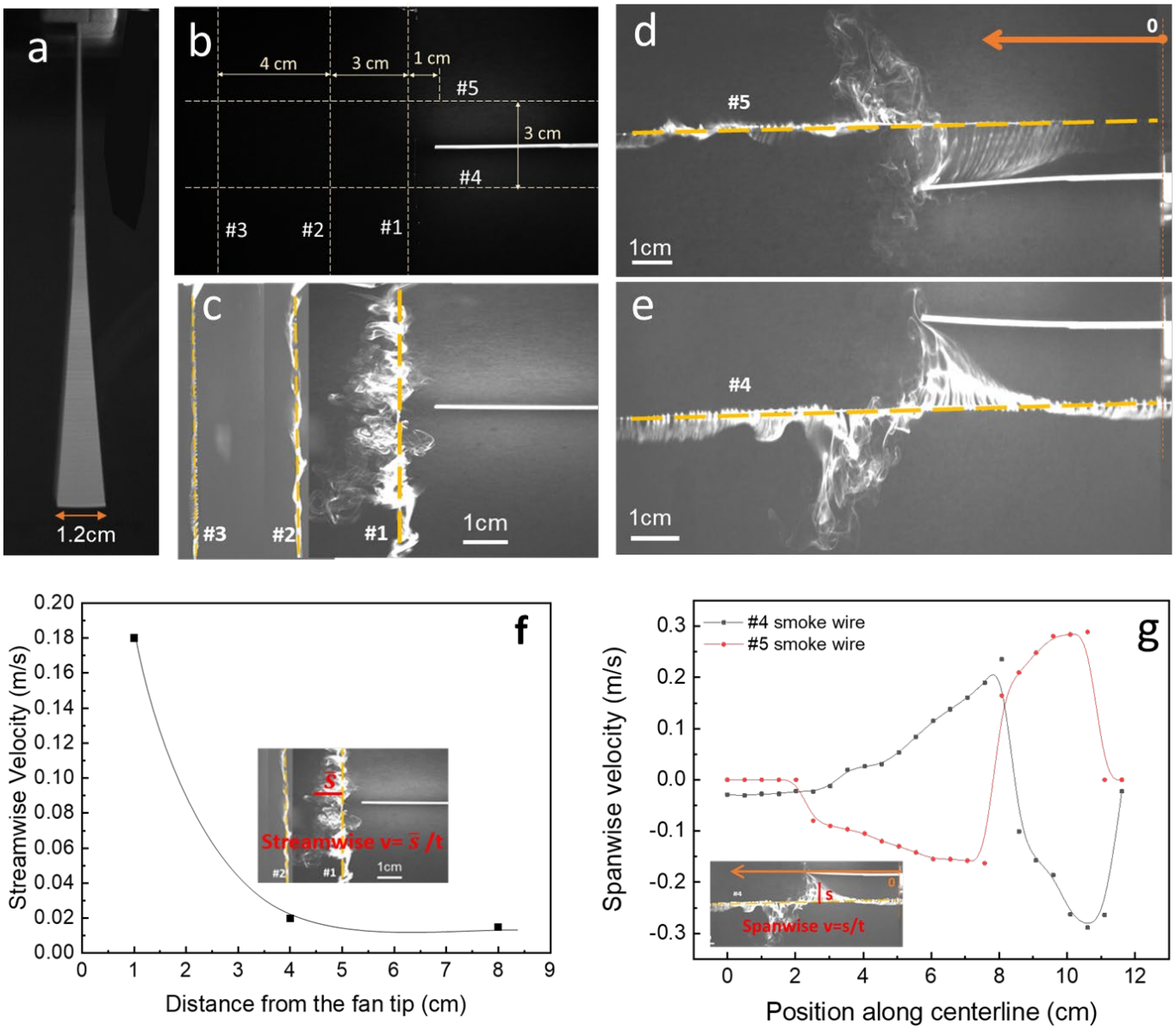

Fig. 2 Flag motion characterization. (a) Flag motion envelope; (b) The relative position of 5 smoke wires to capture the flow patterns around the fan; (c) Flow patterns in front of the fan tip, as shown by smoke wires #1, #2 and #3; Flow patterns parallel to the fan, as shown by smoke wires #4 (d) and #5 (e); (f) Streamwise velocity extracted from (c); (g) Spanwise velocity extracted from (d) and (e).

3.2 The effect of geometrical arrangement on heat transfer

The geometrical optimization in this study consists of two steps. The first step is about the fan position. For cases with different fan positions, Fig. 3(a) shows the heat flux enhancement comparing the piezoelectric fan cooling with the natural convection, while Fig. 3(b) shows the corresponding Nusselt ratios. The effect of the

tip-inlet distance is independent of that of the channel width. When the fan is placed outside the channel (d = 3 cm), the cooling effect is limited compared with other cases. When the fan is gradually inserted into the channel (d = 0 cm, d = -3 cm), the heat flux from the wall gradually increases. However, when the fan is inserted too deep into the channel (d = -6 cm), it can still help the wall cooling, but the effect is diminished. A narrower channel can boost the fan's cooling effect, so the enhanced heat flux induced by the channel with a width of 1.5 cm is higher than the case of 2 cm. However, once the channel is so narrow (the case of 1 cm) that the fan begins to touch the wall during fluttering, the enhancement effect decreases. Therefore, in the first step, the optimized geometrical arrangement for the best cooling effect is to insert the fan into the channel with a distance d = -3 cm while keeping an appropriate channel width w = 1.5 cm. Fig. 3(b) shows that the Nusselt ratio Nu/Nu_0 achieves 1.55 by an optimized configuration. It is supposed that the heat transfer enhancement is related to the streamwise velocity enhancement, which is defined as the channel velocity difference between the natural convection and fan-on condition. The streamwise velocity enhancement was investigated using the direct velocimetry. In the natural convection condition, the outlet velocity is almost 0. When the fan is turned on, the velocity enhancement (Fig. 3(c)) is similar to the results of the heat flux enhancement and Nusselt number ratio (Fig. 3(a) and (b)), except for the case of w = 1 cm. For this case, the fan touches the wall during fluttering, because the fan tip amplitude (1.2 cm) is larger than the channel width (w = 1 cm). The oscillation amplitude of the fan is decreased by the wall, which diminishes the heat transfer performance of the piezoelectric fan. Thus, its heat transfer enhancement effect is sacrificed for the restriction on the fan motion, even though it generates the largest stream velocity enhancement.

The second step for maximizing the heat transfer performance is the channel configuration. When the configuration evolves from an expansion configuration to a normal parallel configuration, then to a contraction configuration, the channel angle evolves from -9.56° to 5.73°. The largest channel angle is 5.73°. For a larger channel angle, the channel outlet will be closed. As shown in Fig. 3(d) and (e), either the expansion configuration or the contraction configuration can boost the heat transfer performance compared with the normal parallel channel. For the expansion configuration, the heat flux enhancement gradually increases firstly and then decreases as the expansion angle increases, i.e., from 0° to -9.56°. At the expansion angle of -5.73°, the heat flux is enhanced by 236 W/m^2, and the Nusselt number is enhanced by 59 %, compared with the case of natural convection. In other words, if this optimized expansion configuration (expansion angle of -5.73°)

is adopted, the piezoelectric fan cooling effect can be enhanced by 60%. For the contraction configuration, the heat flux enhancement has a clear increase and then drops off as the contracting angle increases. The sudden drop is because the forward flow generated by the piezoelectric fan is blocked since the channel outlet is too narrow. The heat flux is enhanced by 250 W/m^2, and the Nusselt number is enhanced by 70%, with a contracting angle of 3.82°. Similarly, if this optimized contraction configuration (contracting angle of 3.82°) is adopted, the piezoelectric fan cooling effect can be enhanced by 70%. The streamwise velocity enhancement using the direct velocimetry method is summarized in Fig. 3(f). The streamwise velocity enhancement increases as the angle evolves from expansion to contraction until the channel outlet is too narrow. The trend is quite different from the heat transfer enhancements in Fig. 3(d) and (e). This suggests that the streamwise velocity enhancement is not the only factor affecting the heat transfer performance. There should exist other mechanisms that have a significant effect on the heat transfer performance.

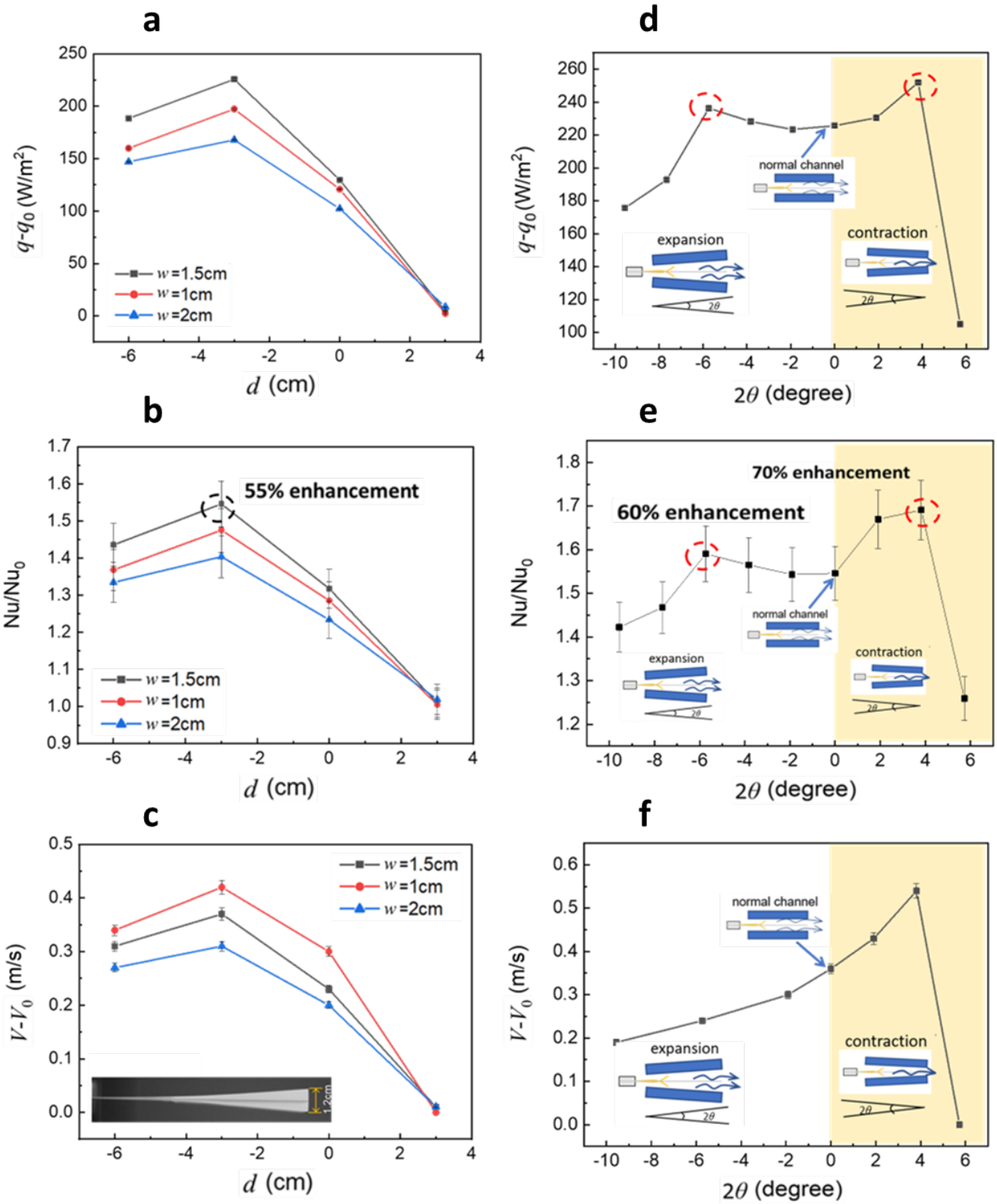

Fig. 3 (a) Heat flux enhancement, (b) Nusselt number ratio and (c) Streamwise velocity enhancement for different d and w; (d) Heat flux enhancement, (e) Nusselt number ratio and (f) Streamwise velocity enhancement for different channel configurations.

3.3 The mechanisms of channel configuration and effects on heat transfer

The expansion or contraction configuration would affect the streamwise and spanwise propagations, which would further affect the heat transfer performance of a piezoelectric fan. Flow visualization is used to investigate this mechanism in this section.

For the contraction configuration, the case of '$2\theta = 3.82°$' can be regarded as a typical case. Two smoke wires were placed at the channel inlet and outlet, respectively. As shown in Fig. 4(a), the flow patterns at the outlet and inlet are shown in the upper figure. The flow at the inlet is mixed quite well and the flow at the outlet shows a jet flow. The outlet flow patterns are different for different angles as shown in the lower three figures in Fig. 4(a). The jet flow is stronger when the contraction angle is larger. Fig. 4(b) shows the velocity profiles at the outlet for different contraction angles. The velocity profiles are all in parabolic shapes but with different amplitudes. Compared with Fig. 2(f), which shows that the streamwise propagation drops rapidly when the distance from the fan tip is larger than 4 cm. Fig. 4(b) reveals that the contraction configuration can further extend the streamwise propagation with a distance of more than 15 cm, covering the channel and extending beyond the outlet. What's more, the streamwise velocity magnitude is also greatly enhanced from 0.18 m/s to 0.7 m/s.

For the expansion configuration, Fig. 5(a) and (b) show the comparison of flow patterns between natural convection (a. fan off) and piezoelectric fan cooling (b. fan on). A smoke wire is placed through the channel, parallel to the channel centerline, showing the flow along the channel. Comparing Fig. 5(a) and (b), clearly, with the fluttering of the piezoelectric fan, air is drawn into the channel and vortices are generated inside. Those vortices propagate along the channel and gradually disappear at a certain distance. What's more, the significant spanwise mixing effect induced by the fluttering of the piezoelectric fan is obviously demonstrated in Fig. 5(b). In the case of '$2\theta = -9.56°$', the vortex propagation length is the shortest. It is also noted that a vortex separation occurs around the end of the fan tip, which will greatly diminish channel air mixing and reduce the heat transfer effect. In the case of '$2\theta = -5.73°$', it has the longest vortex propagation length. The vortices in the inlet area are generated continuously and are the strongest among the three cases. The vortex size becomes bigger and closer to the fan, suggesting the local spanwise mixing effect increases along the

channel direction until reaching the fan tip position. The maximum mixing effect occurs in front of the fan tip, where the air is well-mixed, and then the mixing effect gradually decreases. With the superior streamwise propagation and spanwise mixing, the geometrical arrangement with this optimized expansion angle induced the highest heat transfer enhancement among all expansion configurations. In the case of '2θ = -1.91°', its propagation length is not as long as that in the optimized case, nor strong as its spanwise mixing effect in the inlet area, but still superior to the first case. Its heat transfer performance is accordingly affected. Fig. 5(c) shows the spanwise velocity along the channel centerline, which is extracted from flow patterns in Fig. 5(a) and Fig. 5(b). The spanwise propagation in the area with the piezoelectric fan (centerline position < 3 cm) is similar for different expansion configurations, but different outside that area (centerline position > 3 cm). Outside that area, generally, the '2θ = -5.73°' case has the highest spanwise velocity, while the '2θ = -9.56°' case has the lowest. It is also worth noting that the spanwise velocity intensity is improved from 0.29 m/s, as shown in Fig 2(g), to 0.4 m/s, which benefits the heat transfer. The overall spanwise propagation area is also extracted in Fig. 5(d), indicating the same trend with the Nu/Nu_0 results: the expansion configuration with the better spanwise propagation area obtains the better heat transfer performance.

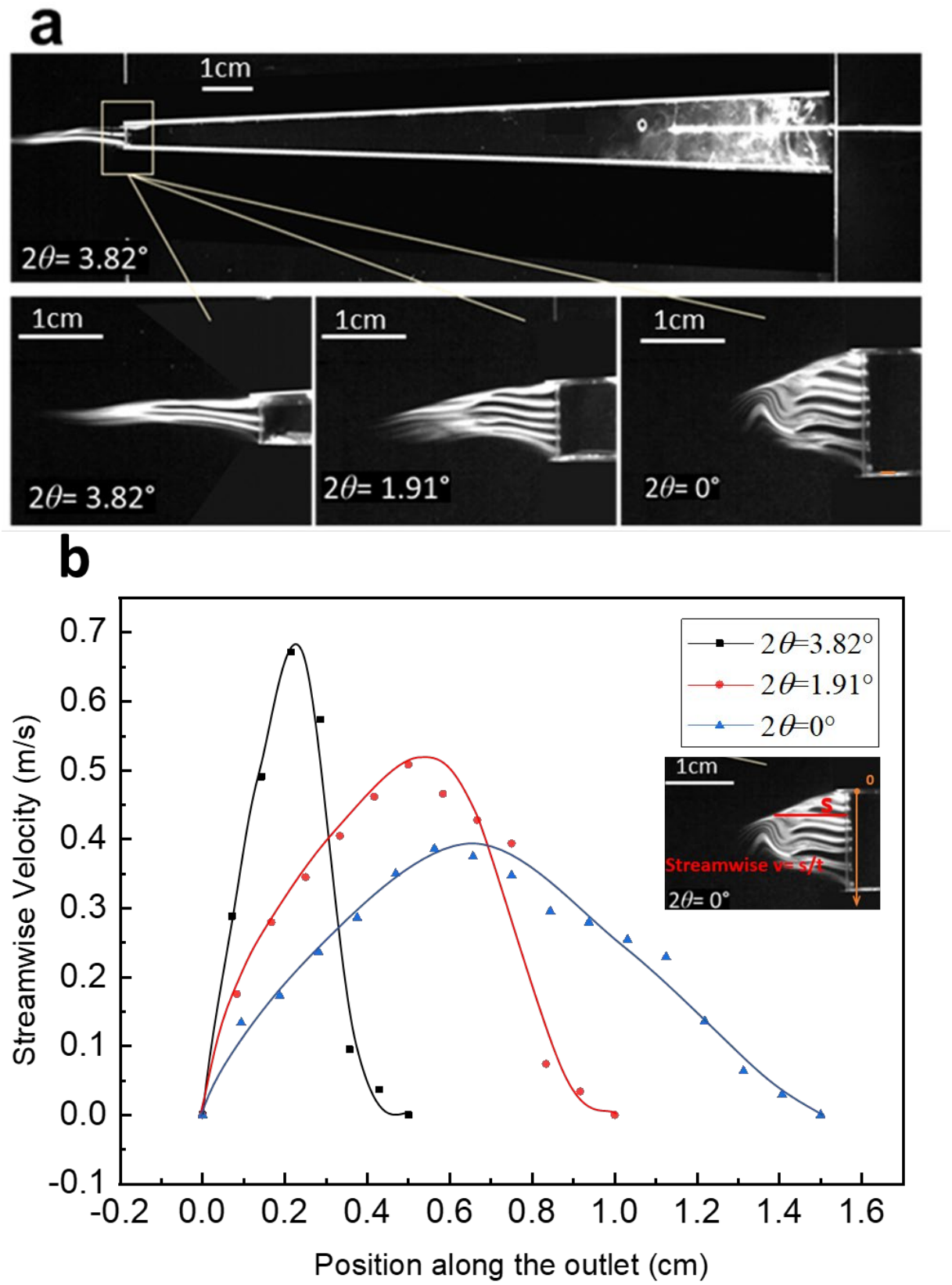

Fig. 4 (a) Flow pattern for contraction configuration; (b) Velocity profiles across the outlet extracted from the flow pattern.

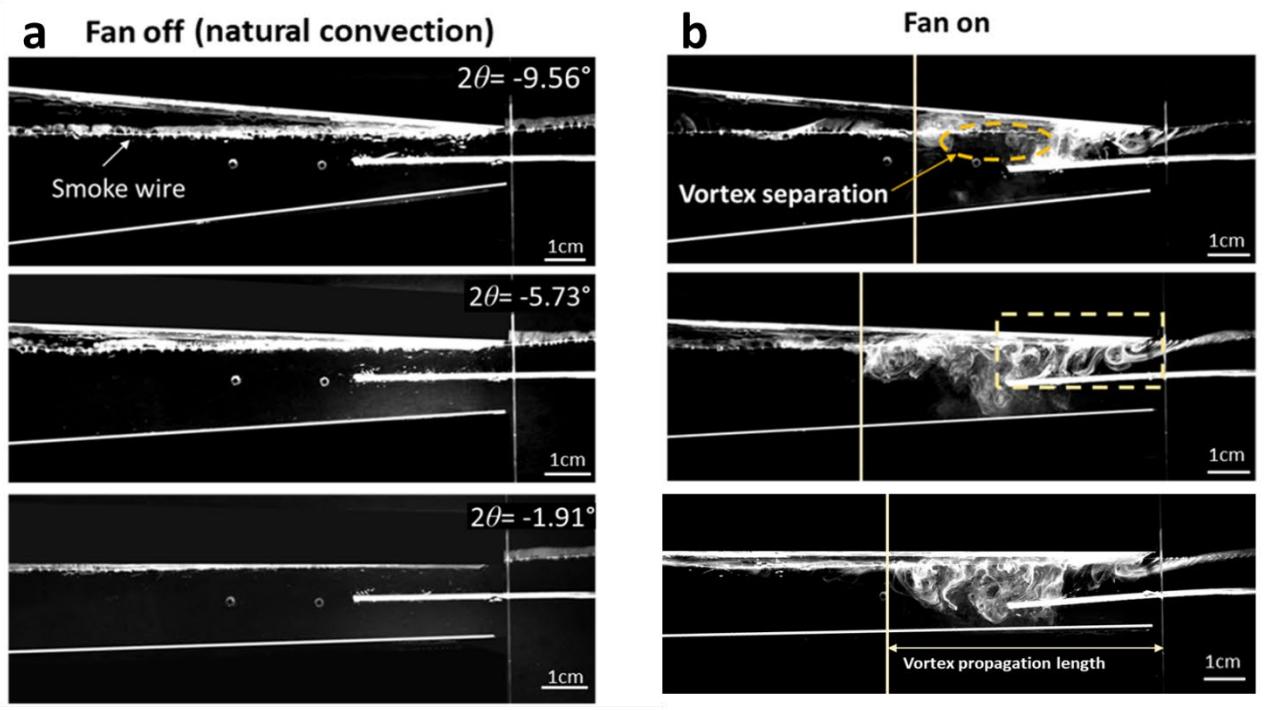

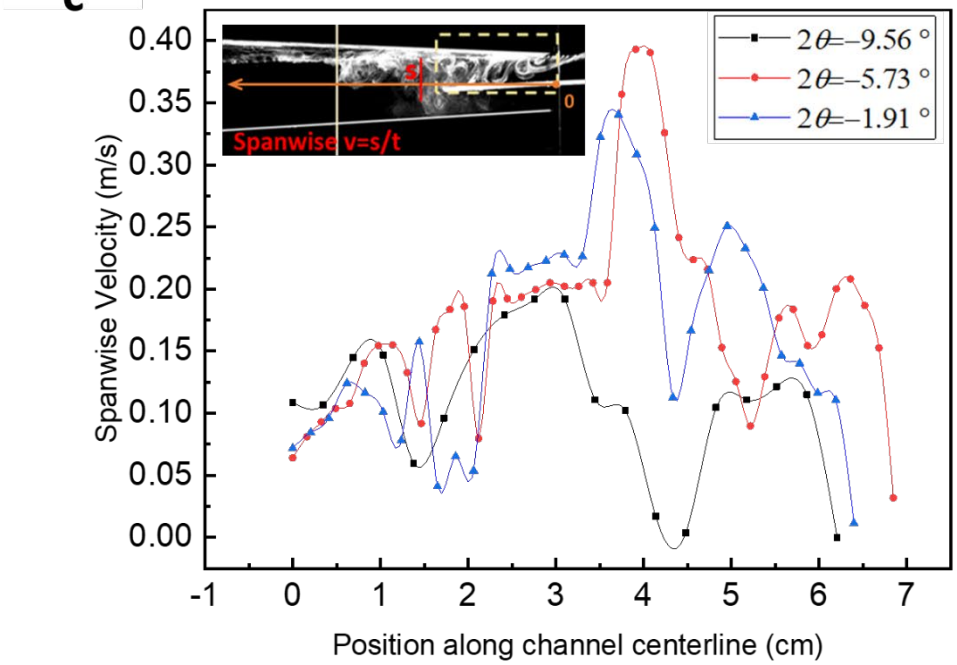

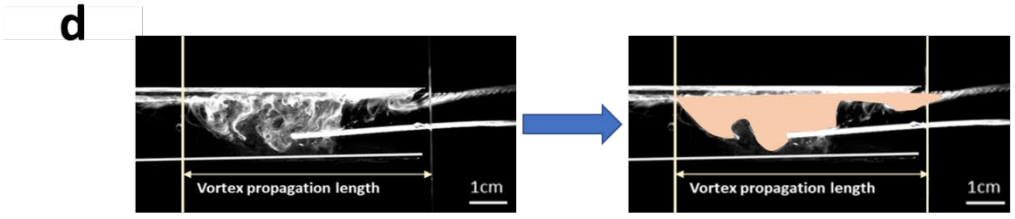

Spanwise propagation area			
Expansion angle	2θ=-9.56°	2θ=-5.73°	2θ=-1.91°
Area (cm^2)	2.76	4.95	4.28

Fig. 5 Flow patterns for expansion configuration, when (a) fan is turned off and when (b) fan is turned on; (c) Spanwise velocity along the channel centerline, extracted from the flow pattern (b); (d) Spanwise propagation area extracted from (b).

4. Concluding Remarks

This work examines the effect of geometrical arrangements on piezoelectric fan cooling. The geometrical optimization consists of two steps, fan position and channel configuration. After optimization, the heat transfer performance is finally enhanced by 70%. Experimental investigation shows that the fan position has a significant effect on the streamwise velocity, thus affecting the overall heat transfer performance. The channel configuration, either expansion or contraction, poses a substantial impact on the flow induced by the fluttering of the piezoelectric fan. In the contraction configurations, jet flow patterns are identified in the channel outlet. In the expansion configurations, vortices with different strengths and propagation distances, as well as vortex separation, are detected. The heat transfer enhancement resulting from the channel configuration is mainly credited to the combination of streamwise propagation and spanwise flow mixing. These geometrical optimizations enhance the cooling performance in the setting with a single piezoelectric fan and a single channel. Future work is recommended to extend the case to multi-fan and/or multi-channel cases. This work offers insight into high-performance piezoelectric fan cooling design and sheds light on future electronic cooling.

5. Acknowledgements

This work was supported by the grants from the Research Grants Council of the Hong Kong Special Administrative Region, China (GRF Project Nos. 17205419 & 17203220). We thank Hanghua Inc. for the equipment support of Smoke-wire Flow Visualization System.

6. References

[1] Y. Guo, X. Zhang, D. Lan, Y. Zhu, Research on heat dissipation performance and long-term reliability of the flapping wing cooling technology applied to the 5G communications equipment, in: 2021 27th International Workshop on Thermal Investigations of ICs and Systems (THERMINIC), IEEE (2021) 1–6.

[2] G. Sacco, S. Pisa, M. Zhadobov, Age-dependence of electromagnetic power and heat deposition in near-surface tissues in emerging 5G bands, Scientific Reports. 11 (2021) 3983.

[3] G. Hetsroni, A. Mosyak, Z. Segal, G. Ziskind, A uniform temperature heat sink for cooling of electronic devices, International Journal of Heat and Mass Transfer. 45 (2002) 3275–3286.

[4] K. Vafai, L. Zhu, Analysis of two-layered micro-channel heat sink concept in electronic cooling, International Journal of Heat and Mass Transfer. 42 (1999) 2287–2297.

[5] S. Sathe, B. Sammakia, A review of recent developments in some practical aspects of air-cooled electronic packages, Journal of Heat Transfer. 120 (1998) 830-839.

[6] J.G. Maveety, J.F. Hendricks, A heat sink performance study considering material, geometry, nozzle placement, and Reynolds number with air impingement, Journal of Electonic Packaging. 121 (1999) 156-161.

[7] W.A. Khan, J.R. Culham, M.M. Yovanovich, The role of fin geometry in heat sink performance, in: ASME 2003 International Electronic Packaging Technical Conference and Exhibition (InterPACK2003), ASME (2003) 279-285.

[8] J. Li, G.P. Peterson, Geometric optimization of a micro heat sink with liquid flow, IEEE Transactions on Components and Packaging Technologies. 29 (2006) 145–154.

[9] D.D. Palande, N.C. Ghuge, G.D. Katale, A comprehensive review on plate heat sink, in: International Conference on Contents, Computing & Communication (ICCCC-2022), SSRN (2022).

[10] B. Agostini, M. Fabbri, J.E. Park, L. Wojtan, J.R. Thome, B. Michel, State of the art of high heat flux cooling technologies, Heat Transfer Engineering. 28 (2007) 258–281.

[11] I. Mudawar, Assessment of high-heat-flux thermal management schemes, IEEE Transactions on Components and Packaging Technologies. 24 (2001) 122–141.

[12] P. Naphon, S. Wiriyasart, Liquid cooling in the mini-rectangular fin heat sink with and without thermoelectric for CPU, International Communications in Heat and Mass Transfer. 36 (2009) 166–171.

[13] H.B. Jang, I. Yoon, C.H. Kim, S. Shin, S.W. Chung, The impact of liquid cooling on 3D multi-core processors, in: 2009 IEEE International Conference on Computer Design, IEEE (2009) 472–478.

[14] C.T. Nguyen, G. Roy, C. Gauthier, N. Galanis, Heat transfer enhancement using Al2O3–water nanofluid for an electronic liquid cooling system, Applied Thermal Engineering. 27 (2007) 1501–1506.

[15] S. Launay, V. Sartre, J. Bonjour, Parametric analysis of loop heat pipe operation: a literature review,

International Journal of Thermal Sciences. 46 (2007) 621–636.

[16] A. Faghri, Review and advances in heat pipe science and technology, Journal of Heat Transfer. 134 (2012)123001.

[17] R.K.B. Gallegos, R.N. Sharma, Flags as vortex generators for heat transfer enhancement: Gaps and challenges, Renewable and Sustainable Energy Reviews. 76 (2017) 950–962.

[18] P. Hidalgo, A. Glezer, Small-scale vorticity induced by a self-oscillating fluttering reed for heat transfer augmentation in air cooled heat sinks, in: International Electronic Packaging Technical Conference and Exhibition, American Society of Mechanical Engineers, (2015)V001T09A004.

[19] M. Maaspuro, Piezoelectric oscillating cantilever fan for thermal management of electronics and LEDs — A review, Microelectronics Reliability. 63 (2016) 342–353.

[20] A. Hales, X. Jiang, A review of piezoelectric fans for low energy cooling of power electronics, Applied Energy. 215 (2018) 321–337.

[21] H.K. Ma, L.K. Tan, Y.T. Li, Investigation of a multiple piezoelectric–magnetic fan system embedded in a heat sink, International Communications in Heat and Mass Transfer. 59 (2014) 166–173.

[22] H.K. Ma, S.K. Liao, C.H. Hsieh, Development of a radial-flow multiple magnetically coupled fan system with one piezoelectric actuator, International Communications in Heat and Mass Transfer. 87 (2017) 212–219.

[23] H.K. Ma, C.H. Hsieh, S.K. Liao, Study of an innovative multiple fan system with one piezoelectric actuator embedded in a circular heat sink, in: 2017 33rd Thermal Measurement, Modeling & Management Symposium (SEMI-THERM), IEEE (2017) 6–12.

[24] Y. Chen, D. Peng, Y. Liu, Heat transfer enhancement of turbulent channel flow using a piezoelectric fan, International Journal of Heat and Mass Transfer. 147 (2020) 118964.

[25] S.F. Liu, R.T. Huang, W.J. Sheu, C.C. Wang, Heat transfer by a piezoelectric fan on a flat surface subject to the influence of horizontal/vertical arrangement, International Journal of Heat and Mass Transfer. 52 (2009) 2565–2570.

[26] L.A. Florio, A. Harnoy, Use of a vibrating plate to enhance natural convection cooling of a discrete heat source in a vertical channel, Applied Thermal Engineering. 27 (2007) 2276–2293.

[27] A. Hales, X. Jiang, Geometric optimisation of piezoelectric fan arrays for low energy cooling, International Journal of Heat and Mass Transfer. 137 (2019) 52–63.

[28] Mide Technology, Forced convection with solid tate piezoelectric fan, https://www.youtube.com/watch?v=LvckweOqjdk&ab_channel=MideTechnology (last accessed by April 28, 2022)

[29] T.L. Bergman, F.P. Incropera, D.P. DeWitt, A.S. Lavine, Fundamentals of heat and mass transfer, seventh ed., John Wiley & Sons (2011).

[30] J. Petroski, M. Arik, M. Gursoy, Optimization of piezoelectric oscillating fan-cooled heat sinks for electronics cooling, IEEE Transactions on Components and Packaging Technologies. 33 (2010) 25–31.

[31] X.L. Zhong, S.C. Fu, K.C. Chan, G. Yang, H.H. Qiu, C.Y.H. Chao, Experimental study on the thermal-hydraulic performance of a fluttering split flag in a channel flow, International Journal of Heat and Mass Transfer. 182 (2022) 121945.

[32] N. Gao, X.H. Liu, An improved smoke-wire flow visualization technique using capacitor as power source, Theoretical and Applied Mechanics Letters. 8 (2018) 378–383.

[33] R.J. Moffat, Describing the uncertainties in experimental results, Experimental Thermal and Fluid Science. 1 (1988) 3–17.